Computers and Electronics in Agriculture 136 (2017) 13–24

Contents lists available at ScienceDirect

Computers and Electronics in Agriculture

journal homepage: www.elsevier.com/locate/compag

Original papers

Analysis of the effects of package design on the rate and uniformity of cooling of stacked pomegranates: Numerical and experimental studies

A. Ambaw [a], Matia Mukama [a], U.L. Opara [a,b,*]

[a] Postharvest Technology Research Laboratory, South African Research Chair in Postharvest Technology, Department of Horticultural Science, Stellenbosch University, Stellenbosch 7602, South Africa

[b] Postharvest Technology Research Laboratory, South African Research Chair in Postharvest Technology, Department of Food Science, Stellenbosch University, Stellenbosch 7602, South Africa

ARTICLE INFO

Article history:
Received 1 November 2016
Accepted 15 February 2017

Keywords:
Forced air cooling
Plastic liners
Postharvest
Cold chain
CFD

ABSTRACT

Computational fluid dynamics (CFD) model was developed, validated and used to analyse cooling characteristics of two different package designs (CT1 and CT2) used for postharvest handling of pomegranate fruit. The model incorporated geometries of fruits, packaging box, tray and plastic liner. Thin layer of plastic material with conservative interface heat flux was used to model liners. The accuracy of the model to predict airflow and temperature distributions were validated against experimental data. The model predicted airflow through the stacks and cooling rates within experimental error. Stack design markedly affected the airflow profile, rate and uniformity of cooling. The cooling rate of the two package designs differed by 30% and plastic lining increased the average 7/8th cooling times from 4.0 and 2.5 h to 9.5 and 8.0 h for the CT1 and CT2 stacks, respectively. Profile of high and low temperature regions depended considerably on packaging box design.

1. Introduction

The demand for pomegranate fruit is increasing due to the extensive knowledge acquired on the health benefits of pomegranate and increased public awareness about functional food (Seeram et al., 2006). Following this, there has been increased interest in research to improve storability (Opara et al., 2015).

Temperature and relative humidity (RH) are important factors that control respiratory activity, physiological disorders and growth of microbial pathogens during storage of pomegranate fruit (Munhuweyi et al., 2016; Pareek et al., 2015). Optimum storage temperature varies by cultivar, production area, and postharvest treatment (Köksal, 1989; Onur et al., 1995). Normally, storage is recommended at temperatures between 5 °C and 8 °C (Artés et al., 1996; Fawole and Opara, 2013; Kader et al., 1984) and relative humidity (RH) between 90 and 95% (Artés et al., 1996; Mirdehghan et al., 2007). After harvest, produce normally contain heat from the field (field heat) and fruit temperature is higher than the recommendation. Hence, it is necessary to remove the field heat to bring the harvested produce to the storage temperature by employing a precooling process. After precooling, commodity should be maintained at its lowest safe temperature.

Precooling of pomegranate can be accomplished using room cooling. In this technique, stacked fruit are placed in an insulated room equipped with refrigeration units to chill the air. However, room cooling is a slow process. Forced-air cooling (FAC) system uses fan to drive cold air through stacked produce to increase the rate of convective heat transfer from the commodity to the cooling medium. Hence, FAC is the most commonly used technique in postharvest precooling of fruits and vegetables. FAC can be used in conjunction with cold storage room. Fresh harvest can be rapidly precooled to the required storage temperature and then transferred to cool store room. This helps to maintain the cool room environment constant.

There are many factors that affect the effectiveness of precooling of perishables (Opara and Zou, 2007; Zou et al., 2006a,b). Among these, the role of package design and package arrangement on uniformity and rate of cooling have been highlighted by many researchers (Berry et al., 2015, 2016; Defraeye et al., 2013; Delele et al., 2013; Ngcobo et al., 2012; Opara, 2011). Size, proportion and locations of vent-holes on top, bottom and side faces of a packaging box considerably affect cooling rate and uniformity (Berry et al., 2015, 2016). Plastic liner is commonly used to reduce moisture loss and to control gas compositions (CO2 and O2) during storage (Mangaraj et al., 2009; Opara, 2011). However, plastic liner also

* Corresponding author at: Postharvest Technology Research Laboratory, South African Research Chair in Postharvest Technology, Department of Horticultural Science, Stellenbosch University, Stellenbosch 7602, South Africa.
E-mail addresses: opara@sun.ac.za, umunam@yahoo.co.uk (U.L. Opara).

http://dx.doi.org/10.1016/j.compag.2017.02.015
0168-1699/

blocks airflow and reduces the rate of heat removal from the produce. Understanding the influence of package designs on the rate and uniformity of cooling helps to optimize the process.

Such knowledge can be acquired experimentally. Here, spatiotemporal temperature data can be processed to estimate cooling coefficients, 7/8th cooling time and cooling uniformities (Anderson et al., 2004; Gil et al., 2012; Akdemir and Arin, 2006). However, experimental approach alone is expensive, time taking and inconvenient to perform detailed analysis of airflow and temperature distributions. By combining experimental measurements with mathematical models, a more comprehensive analysis can be realised (Verboven et al., 2006; Zou et al., 2006a,b; Alvarez and Flick, 1999a,b; Ferrua and Singh, 2009). The powerful visualization capabilities and acceptable accuracy of the numerical predictions make computational fluid dynamics (CFD) the primary method of choice in modelling mass and heat transfer processes (Ambaw et al., 2013; Norton and Da-Wen, 2006; Smale et al., 2006).

While research on the health benefits (Mertens-Talcott et al., 2006; Viuda-Martos et al., 2010) and improved postharvest handling methods (Artés et al., 2000; Mirdehghan et al., 2006; Opara et al., 2015) has been reported, little is known about precooling of pomegranate fruit in the cold chain. Direct extrapolation from studies on other fruit types is not appropriate since thermal properties, package designs, package arrangement and precooling requirements are specific.

The aim of the present work is to examine the aerodynamic and thermodynamic performances of two different corrugated fibreboard containers to handle 'Wonderful' pomegranate fruit with or without plastic liner. To accomplish this, CFD models were developed and validated. Then, the validated model was used to analyse the airflow and temperature distributions with very high spatial resolution.

2. Materials and methods

2.1. Fruits

Pomegranate fruit (Punica granatum L., cv. Wonderful) was harvested at commercial maturity from Merwespont farm in Bonnievale, Western Cape, South Africa. Fruits were transported in an air-conditioned vehicle to Postharvest Technology Research Laboratory in Stellenbosch University. The average size of pomegranates were 8.00 ± 0.20 cm in diameter and 358 ± 10 g in mass. Before the start of the experiments fruits were equilibrated to ambient air temperature which was17 ± 3.0 °C.

2.2. Packaging boxes

Two corrugated packaging box designs (CT1 and CT2) were examined in this study. Each box design carry twelve pomegranate fruits (fruit only Fig. 1(a) and fruit enveloped in plastic liner Fig. 1 (b)). Table 1 summarizes the loading capacities and vent area characteristics of the boxes. Plastic wrapping was done by placing pomegranates in a single non-perforated 10 μm thick high density polyethylene (HDPE) plastic film (Fig. 1(b)). The dimensions and vent-hole locations of the two boxes are presented in Fig. 2.

Fig. 1. Components of the experimental setup. Pomegranates in the CT2 packaging box, with no lining (a), with liner (b), thermocouple inserted to fruit centre to measure pulp temperature (c) and stack ready for the FAC test (d).

2.3. Precooling experiments

Boxes were stacked on a standard ISO industrial pallet (1.2 × 1.0 m × 0.1 m) (Fig. 2(e) and (f)). The CT1 stack holds 7 layers of 10 boxes while the CT2 stack holds 8 layers of 12 boxes. Then each stack was individually placed in front of the FAC system inside cold storage room. The top, left and right sides of the stack were carefully sealed with plastic sheet (Fig. 1(e)). The FAC system uses centrifugal fan (Kruger KDD 10/10 750W 4P-1 3SY) to draw cold air through the stack. Temperature and relative humidity (RH) of the cold store room were 7 ± 1.2 °C and 91.4 ± 6.3%, respectively. Pressure at inlet and outlet and air velocity at outlet of the FAC system were measured using differential pressure meter (Air Flow Meter Type A2G-25/air2guide, Wika, Lawrenceville GA 30043, USA with a long-term stability of ±1 Pa) with data controller (WCS-13A, Shinko Technos CO LTD, Osaka, Japan).

Fruit pulp temperatures were measured by inserting T-type thermocouple into the core of sample fruits (Fig. 1(c)). The thermocouple used has operating range of −30 to 100 °C and accuracy of ±0.025% (Thermocouple products Ltd, Edenvale, South Africa). The interference due to the physical presence of a thermocouple inside fruit (due to their heat capacity and density) was assumed negligible as the thermocouples were small in size compared to the fruit. The relative positions of the temperature sensors in a layer is

Table 1
Package dimensions, vent-hole ratios and loadings.

Models	Dimensions [m]	Vent hole ratio [%]			Loading	
		Short side	Long side	Bottom side	Number of fruits	Total weight [kg]
CT1	0.39 × 0.29 × 0.12	2.0	8.0	3.0	12	4.3
CT2	0.33 × 0.30 × 0.11	5.3[a]	10.20	3.8	12	4.3

[a] Not that during stacking this vent-hole would be blocked. In a stack, this side has practically no vent-hole.

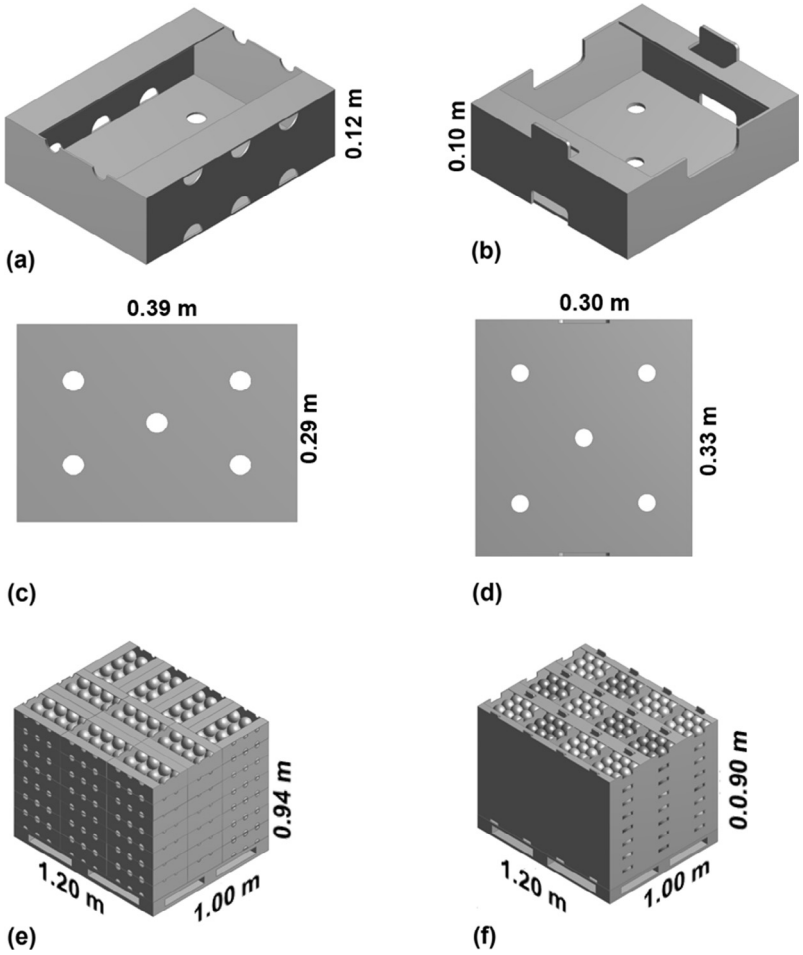

Fig. 2. Schematics of the two package designs. The top row shows the isometric view of the CT1 (a) and CT2 (b) boxes. The middle row show vent holes on the bottom side of the CT1 (c) and CT2 (d) boxes, respectively. The bottom row depicts dimensions and box orientation of the CT1 (e) and CT2 (f) packages stacked on a standard ISO industrial pallet.

shown in Fig. 3. Sampling fruits were placed in layers: 2, 4 and 6 of the stacks. This way pulp temperature data were collected every 300 s.

2.4. Model formulation

2.4.1. Model assumptions

The CFD model was developed based on the following assumptions:

- Pomegranates are spherical with uniform diameter (80 mm) and ideally arranged inside a box.
- Thermal properties of pomegranate fruit was estimated using models for food components (Choi and Okos, 1986) at average fruit pulp temperature of 12 °C and mass composition of: 80.97% moisture, 0.95% protein, 0.30% fat, 16.57% carbohydrate, 0.6% fibre and 0.61% ash (USDA, 1996).
- The influence of moisture loss on the energy balance was assumed negligible and thus not included in the model.
- Mass transfer across the plastic liner was assumed negligible. However, the heat transfer across the interface separating the free air and the air inside the liner was modelled.
- Thermal property of cardboard obtained from Ho et al. (2010) were used in the model. The actual values of our carton may have some difference from the values used in the model.

Table 2 summarizes the material property data used in the CFD model.

2.4.2. Governing equations

The airflow was modelled by the Reynolds Averaged Navier Stokes (RANS) equations with the continuity, momentum, and energy balance equations as given in Eqs. (1)–(3), respectively.

$$\nabla \cdot \mathbf{u} = 0 \tag{1}$$

$$\frac{\partial(\mathbf{u})}{\partial t} + \nabla \cdot ((\mathbf{u} \otimes \mathbf{u})) - \nabla \cdot \left(\left(\frac{\mu + \mu_t}{\rho_a} \right) \nabla \mathbf{u} \right) = \mathbf{S}_U - \frac{1}{\rho_a} \nabla p \tag{2}$$

$$(\rho_a C_{pa}) \left(\frac{\partial T_a}{\partial t} + \mathbf{u} \cdot \nabla T_a \right) = \nabla \cdot ((k_a + k_t) \nabla T_a) + Q_a \tag{3}$$

where $\mathbf{u}$ is the vector of the velocity (m/s), t is time (s), μ is the dynamic viscosity of air (kg m^{-1} s^{-1}), μ_t is the turbulent eddy viscosity (kg m^{-1} s^{-1}), p is pressure (Pa) and $\mathbf{S}_U$ (m/s^2) is the momentum source term, C_{pa} (J kg^{-1} K^{-1}) is the heat capacity of air, ρ_a (kg m^{-3}) is the density of air, ρ_s (kg m^{-3}) is the density of apple fruit, T_a (K) is the air temperature, k_a(W m^{-1} K^{-1}) is the thermal conductivity of air, k_t (W m^{-1} K^{-1}) is the turbulent thermal conductivity. The turbulent thermal conductivity is a function of the turbulent viscosity, the heat capacity and Prandtl number of air and calculate using the shear stress transport (SST) k-ω turbulence

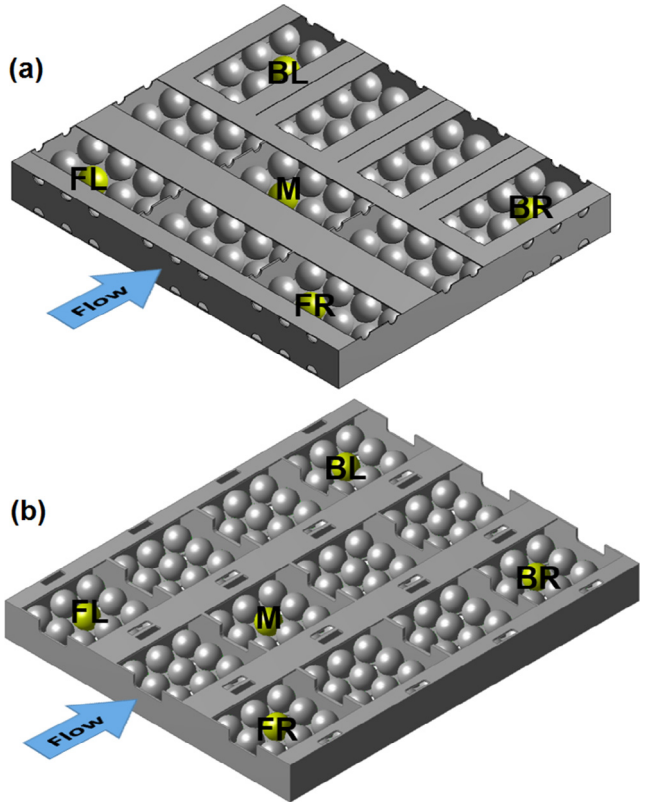

Fig. 3. Positions of thermocouples in a layer of the CT1 (a) and CT2 (b) stacks. Thermocouples were placed in Layers: 2, 4 and 6 of the stack at the front left (FL), front right (FR), middle (M), and back left (BL) and back right (BR) boxes.

model (Defraeye et al., 2013; Delele et al., 2008, 2013; Menter, 1994). In the fruit the heat transfer is given by Eq. (4)

$$(\rho_s C_{ps})\left(\frac{\partial T_s}{\partial t}\right) = \nabla \cdot (k_s \nabla T_s) + Q_s \quad (4)$$

where ρ_s (kg m^{-3}) is the density of pomegranate fruit, C_{ps} (J kg^{-1} K^{-1}) is the heat capacity of pomegranate fruit, T_s (K) is the produce temperature, k_s (W m^{-1} K^{-1}) is the thermal conductivity of pomegranate fruit. Pomegranate is a non-climacteric fruit and has a relatively low respiration rate that declines with time during storage after harvest (Fawole and Opara, 2013; Kader et al., 1984). Hence, the heat of respiration Q_s (W m^{-3}) in Eq. (4) was assumed negligible in the model. The main model parameters and their values are summarized in Table 2.

2.4.3. Geometry and boundary conditions

Spheres representing pomegranate fruits, detailed design of boxes, tray (for the CT1 stack), plastic liner and the FAC system were replicated in the CFD model. In the CT1 box fruits were placed on a tray with depressions to position individual fruit. Whereas the CT2 box has no tray and fruits were directly placed in the box.

Steady state airflow and pressure distributions were modelled for the full stack. Fig. 4 illustrates the model geometry and boundary conditions of the problem. The plastic liner separating the free air and the air inside liner were modelled as a no slip wall of thin plastic material (10 μm) with conservative heat flux defined based on thermal properties of HDPE material. Fruit surfaces and box surfaces were set to wall, no-slip boundaries with respect to airflow and to conservative flux for heat transfer. The inlet to the domain was open to the atmosphere (at atmospheric pressure) and the outlet of the domain, which corresponds to the inlet to the suction fan, was at suction pressure (negative gauge pressure).

2.4.4. Simulation setup

Geometry creation, domain discretization and numerical simulations were performed with the CFD code on ANSYS®CFX™ Release 17.0 (ANSYS, Canonsburg, PA, USA). Mesh dependency was analysed based on the difference in values of air velocity in the full stack model for grid sizes of 4×10^6, 8×10^6 and 12×10^6 elements. For this purpose, air velocities through vent holes at the inlet side of the stack were computed and average discretization error was estimated using the Richardson extrapolation method (Franke et al., 2007; Roache, 1994). The actual simulations were finally undertaken using 10×10^6 elements which had an average discretization error in estimating air velocity of 2.6%.

Solving the heat transfer problem required a very fine mesh to accurately capture the interfacial heat fluxes. Modelling this problem on the full stack was computationally difficult and time taking. A pre-assessment of the temperature measurement data revelled a nearly uniform cooling rate across each layer of a stack. Additionally, simulated airflow and pressure fields for the full stack showed similar distribution across each layer of a stack. Hence, in this study, the transient heat transfer problem was solved for a single layer, taken out of the stack (Fig. 5). For the single layer model, mesh dependency was analysed using fruit pulp temperature as criterion giving a mesh elements of 2×10^6.

SIMPLE discretization scheme was used for pressure-velocity coupling and Second Order Upwind discretization was used for momentum, specific dissipation rate and energy calculations. A number of time step sizes (360 s, 180 s, 72 s, 36 s) were assessed. Based on accuracy and computational time, time step size of 180 s with maximum 10 iterations per time step, was used. Simulation were run on a 64-bit, Intel(R) Xeon(R) CPU E5-1660 v3, 3 GHz, 32 Gb RAM, Windows 7 PC.

Table 2
Material properties and their values.

Parameters	Value	Reference
Density of plastic liner (HDPE) (ρ_L)	959 kg/m^3	Harper (2004)
Density of pomegranate (ρ_p)	1135 kg/m^3	Estimated
Density of cardboard (ρ_{cb})[a]	145 kg/m^3	Ho et al. (2010)
Heat capacity of plastic liner (HDPE) (c_{pL})	2000 J/kg K	Harper (2004)
Heat capacity of pomegranate (c_{ps})[b]	3645 J/kg K	Choi and Okos (1986)
Heat capacity of cardboard (c_{cb})	1338 J/kg K	Ho et al. (2010)
Mean fruit diameter (d)	0.080 m	Measured
Thermal conductivity of pomegranate (k_p)[b]	0.52 W/mK	Choi and Okos (1986)
Thermal conductivity of plastic liner (HDPE) (k_L)	0.43 W/mK	Harper (2004)
Thermal conductivity of cardboard (k_{cb})	0.064 W/mK	Ho et al. (2010)

[a] Property of cardboard obtained from Ho et al. (2010) were used in the model. The actual values of our carton may have some difference from the values used in the model.
[b] Thermal properties of pomegranate fruit was estimated using thermal property models for food components at average fruit pulp temperature of 12 °C (Choi and Okos, 1986) and with mass composition of pomegranate fruit: 80.97% moisture, 0.95% protein, 0.30% fat, 16.57% carbohydrate, 0.6% fibre and 0.61% ash (USDA, 1996).

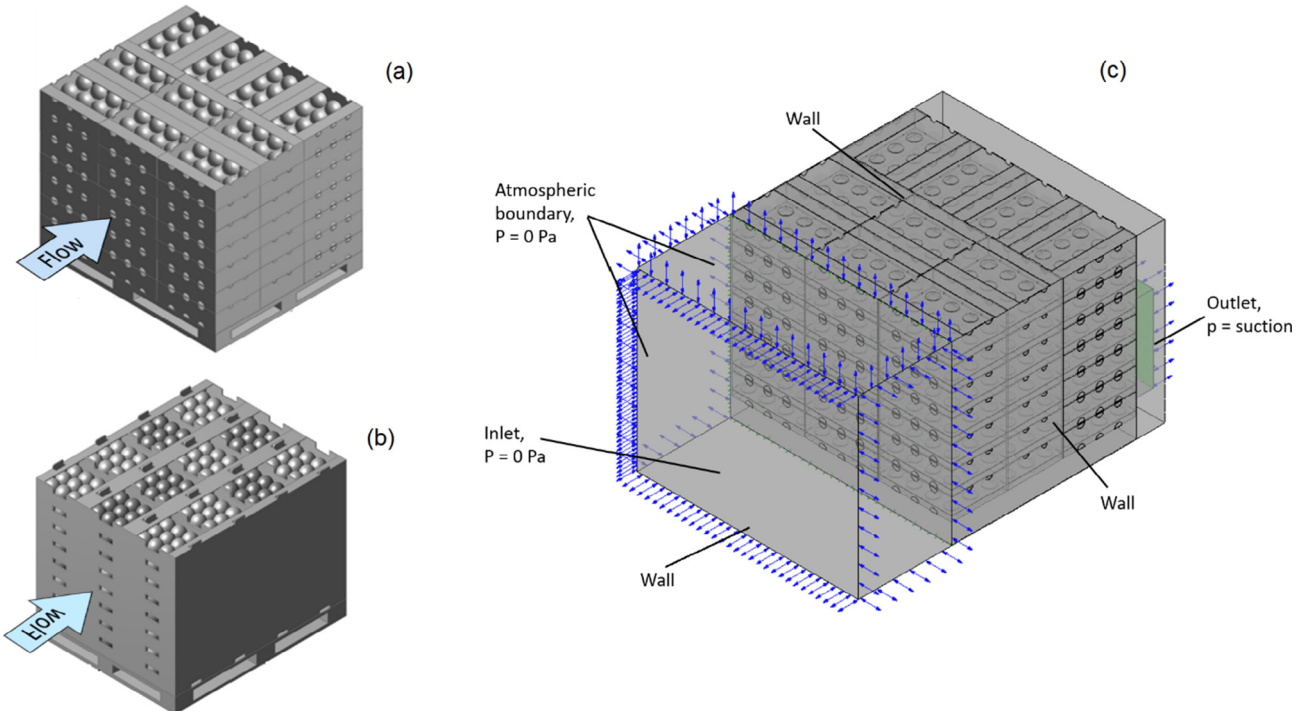

Fig. 4. Schematics showing the stack and the airflow direction tested on the CT1 stack (a), CT2 stack (b) and illustration of the computational domain and boundary conditions of the model for the airflow distribution (c).

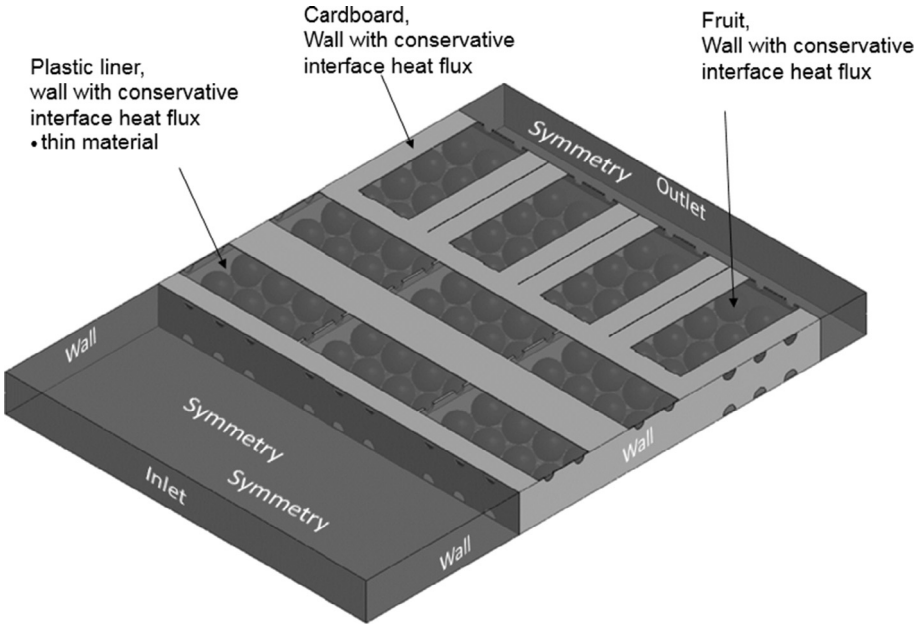

Fig. 5. Schematics showing boundary conditions used to simulate the transient heat transfer problem. The layer corresponds to the CT1 stacked.

3. Results and discussions

3.1. Model validation

Validation of the CFD model was done by comparing computed and experimentally obtained airflow, pressure drop and temperature data. The experimental uncertainty was calculated from standard deviation of measurements from three repeated experiments.

3.1.1. Pressure drop characteristics

The measured and simulated pressure drop vs. flow rate data of the CT1 and CT2 stacks are presented in Fig. 6. As expected, pressure loss is affected by package design and plastic liners. CT2 stack with no liner (CT2_No lining) has the lowest pressure loss while CT2 box with liner (CT2_With lining) has the highest loss. The CT1 stack has intermediate pressure loss characteristics.

The CFD model captured the pressure drop characteristics within the measurement error. Simulated values were, in average, 15% higher than measured values (curves in Fig. 6). Gaps between boxes and between the stack and the stack covers are completely avoided in the model. In actual case, such gaps are inevitable and air can leak through such gaps.

Superficial air velocity depends on the permeability of the stack, the flowing fluid (air) properties and the pressure gradient applied

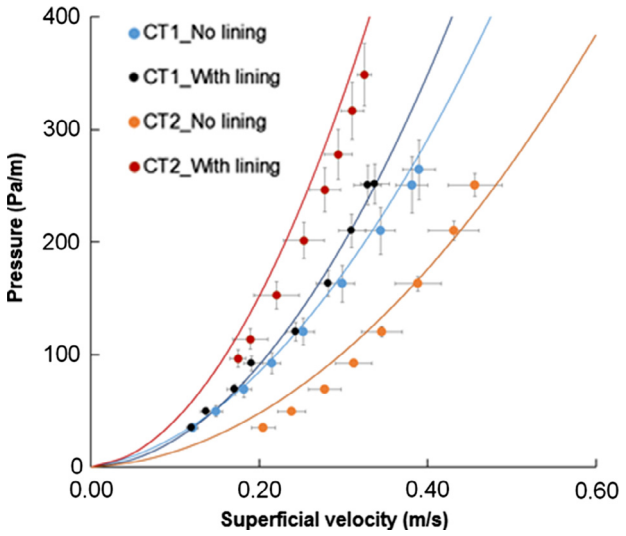

Fig. 6. Measured (dots) and simulated (curves) pressure drop across the stacks as a function of superficial air velocity through the stack. Horizontal and vertical lines corresponds to standard deviation of three repeated superficial air velocity and pressure drop measurements, respectively.

for air delivery. This relationship was captured using the Darcy-Forchheimer equation (Eq. (5)).

$$M_V = -\frac{\mu}{k}V - \frac{\rho}{k_1}|V|V \tag{5}$$

where V (m/s) is superficial velocity, defined as the volumetric flow rate divided by the cross sectional area of the stack perpendicular to the flow direction. The coefficient μ/k (Darcy term) accounts for friction losses that are characteristics of the fluid viscosity μ (Pa s) and the permeability of the stack k (m^2). The coefficient ρ/k_1 takes into account inertial losses associated with expansion, constriction, and bends in the pore channels where the additional term k_1 (m) is known as inertial permeability. Fitting the pressure drop vs. velocity data to Eq. (5) give pressure loss coefficients of the stacks (Table 3). Simulated and measured coefficients agree very well with respect to the inertial loss coefficient (ρ/k_1). This coefficient is dominant at high airflow due to inertial effects (Verboven et al., 2006). Plastic liner influences the CT2 stack most. For this stack, plastic liner increased the pressure drop by 3-fold. In the contrary, the influence of plastic liner in the CT1 stack was relatively small, it increased the resistance by 27%. The vent holes of the CT1 container were many in number and spread on the box sides. However, in the CT2 stack, the single vent hole on the top rim of the box could be easily blocked by plastic liner.

3.1.2. Cooling rates

Initial pulp temperatures were slightly different between experiments, also between sampling fruits at different location in the stack. Hence, to compare the cooling rate at equal ground, a dimensionless parameter, as given by Eq. (6), was used. This equation describes the cooling rate in terms of the fractional unaccomplished temperature change Y (Defraeye et al., 2013).

$$Y = \frac{T - T_a}{T_i - T_a} \tag{6}$$

where T is the measure pulp temperature (°C), T_a is the cooling air temperature, which was taken to be the set point temperature of the cooling unit ≈7 °C and T_i is the initial pulp temperature of the produce (°C). Fig. 7 depicted the measured and simulated time-temperature curves per layer. Cooling rate significantly affected by plastic lining as can be confirmed by the clearly grouped curves of stack without lining (broken curves) and stack with lining (full curves). The model (full black curve) approximated cooling rate with slight underestimation. The underestimation of the cooling rate was, in part, due to the constant value of cooling air temperature (7 °C) used in the simulation. In actual case the cool room temperature was often lower than 7 °C. In addition, for stacks with plastic liners, the model may not accurately reproduced the actual position of plastic liner with respect to pomegranates. To get a robust and computationally stable simulation, plastic liner was positioned 2 mm away from the pomegranate fruits to simplify

Table 3
Comparison of simulated and measured pressure loss coefficients of the different packages.

		μ/k (Pa s m^{-2})		ρ/k_1 (kg m^{-4})	
		Model	Experiment	Model	Experiment
With liner	CT1	30.88	36.88	2088.80	2078.88
	CT2	76.60	8.02	3420.00	3507.00
No liner	CT1	120.69	1.80	1520.10	1563.40
	CT2	40.00	1.86	1000.40	1563.40

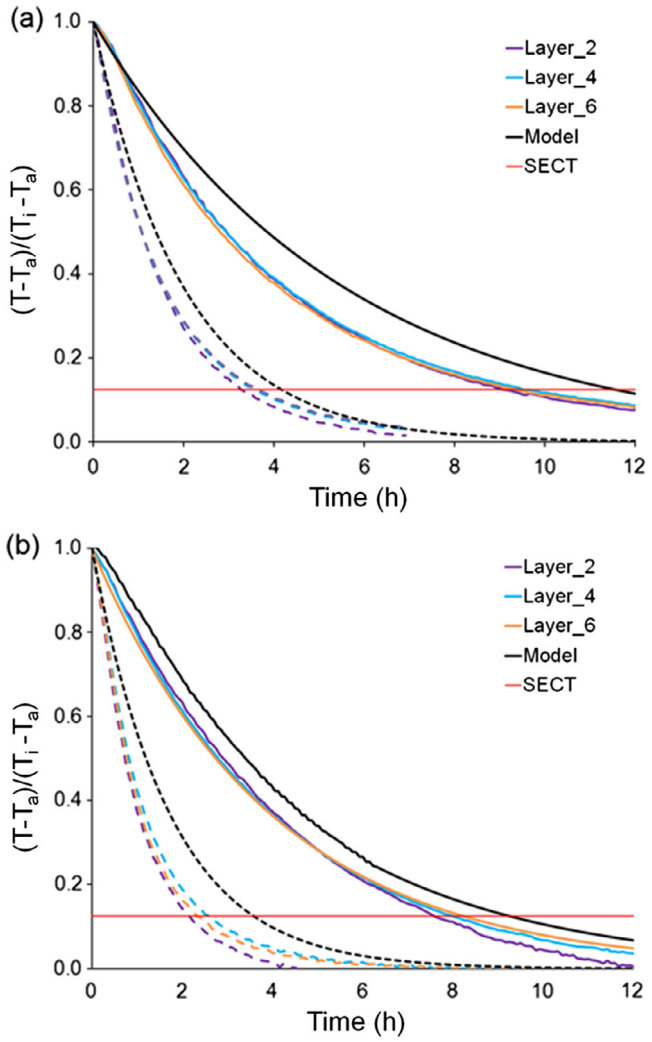

Fig. 7. Layer average time-temperature curves for a stack with lining (full curves) and no lining (broken curves) of CT1 (a) and CT2 (b). Simulated values, obtained from a single layer model are shown in black color. T_a = 7 °C was used in the normalizing equation. Measurements and simulations correspond were at air flow rate of 0.5 L kg^{-1} s^{-1}.

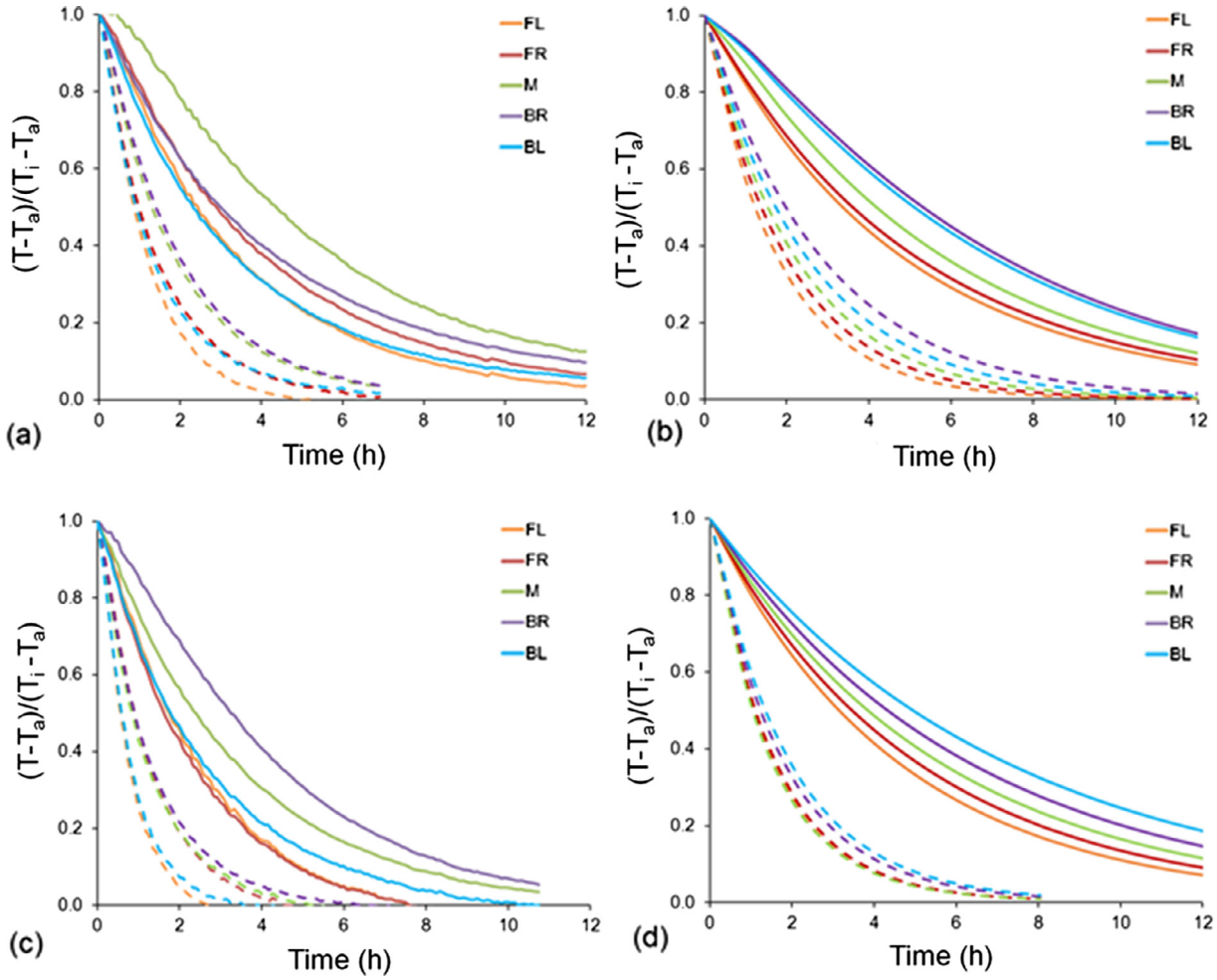

Fig. 8. Measured ((a) and (c)) and simulated ((b) and (d)) average pulp temperature histories per sample position in CT1 ((a) and (b)) and CT2 ((c) and (d)) boxes, with lining (full curves) and no lining (broken curves). T_a = 7 °C was used in the normalizing equation. Measurements and simulations correspond to an airflow rate of 0.5 L kg^{-1} s^{-1}.

the grid generation. This creates insulating air layer between the plastic liner and the fruit, reducing the heat transfer rates. Notice that the time-temperature curves of layers in a given stack were nearly identical for all the cases.

Fig. 8 depicts layer averaged time-temperature curves of sample pomegranate fruits (see Fig. 3 for sample positions). The experimental result showed cooling rate magnitude arranged as FL > BL > FR > M > BR. Clearly, temperature non-uniformity was high between fruits in different boxes in a layer. Pomegranate fruits in boxes at the front region of the stack were receiving cooling air first, and its boundaries are adjacent to the cold air of the cool store room. Fruits in the middle and especially those in the back received warmer air infiltrated through fruits in the front region. Hence, boxes in the front region (FL and FR) are normally expected to cool faster followed by boxes in the middle region and then fruits in the back region of a stack. However, the experiment didn't go in parallel with the expectation and didn't show a coherent trend to describe the variation. For the CT1 stack with lining the middle stack (M) was observed to have the lowest cooling rate. The cause of deviation from expectation may be due to the cold air distribution in the cool store room. Also, air leaving the FAC system may interact with airflow from the cooling unit of the cold storage room, creating a non-uniform air temperature at inlet to the FAC system. The CFD model (Fig. 8(b) and (d)), however, followed the expected trend of temperature distribution.

Table 4 summarizes the result of simulated and measured 7/8th cooling times (SECTs) of precooling of the different packages. Predicted cooling times were at max 20% higher than measurements. The difference between the two package designs were more significant in cases of no liners, here cooling rate of the two package designs differed by more than 30% and plastic lining increased the average 7/8th cooling times from 3.5 and 2.5 h to 9.5 and 8.0 h for the CT1 and CT2 stacks, respectively.

3.2. Analysis of pressure loss and airflow distributions

Fig. 9 depicts simulated profiles of pressure distribution in the stack. The contour plots and the graphs clearly identified locations of major pressure loses in the stacks. For the CT1 stack the most

Table 4
SECT of the CT1 and CT2 stacks at cooling air (7 °C) flow rate of 0.5 L kg^{-1} s^{-1}.

		SECT (h)	
		Model	Experiment
With liner	CT1	11.5	9.5
	CT2	9.3	8.0
No liner	CT1	4.2	3.5
	CT2	3.7	2.5

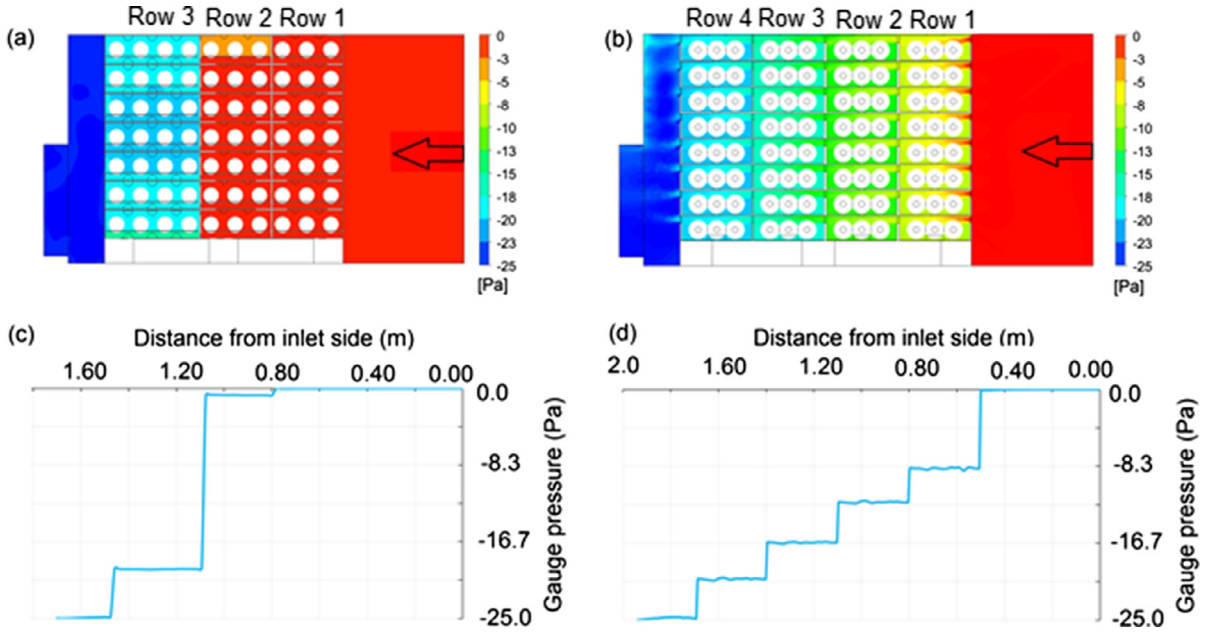

Fig. 9. Simulated contour of pressure distribution on vertical plane sectioning the CT1 (a) and CT2 (b) stacks. The pressure gradient along horizontal line passing through the CT1 (c) and CT2 (d) stacks. Simulations were at airflow rate of 0.5 L kg^{-1} s^{-1}.

important location was between row 2 and row 3. At this junction, pressure dropped by 20 Pa (≈80% of the overall pressure gradient). For the CT2 stack, pressure dropped by about 8 Pa (≈32%) at inlet to the stack, then flow from one box to another causes a 5 Pa drop (≈20%). The pressure field stayed constant inside a box for both stacks. Normally, in postharvest handling of pomegranates, small numbers of fruits are loaded in a box in single layer and are loosely packed. Due to this, the resistance to airflow due to the pomegranate fruits in a box is negligible and that across vent holes of the packaging box is important. This is in contrast to handling other

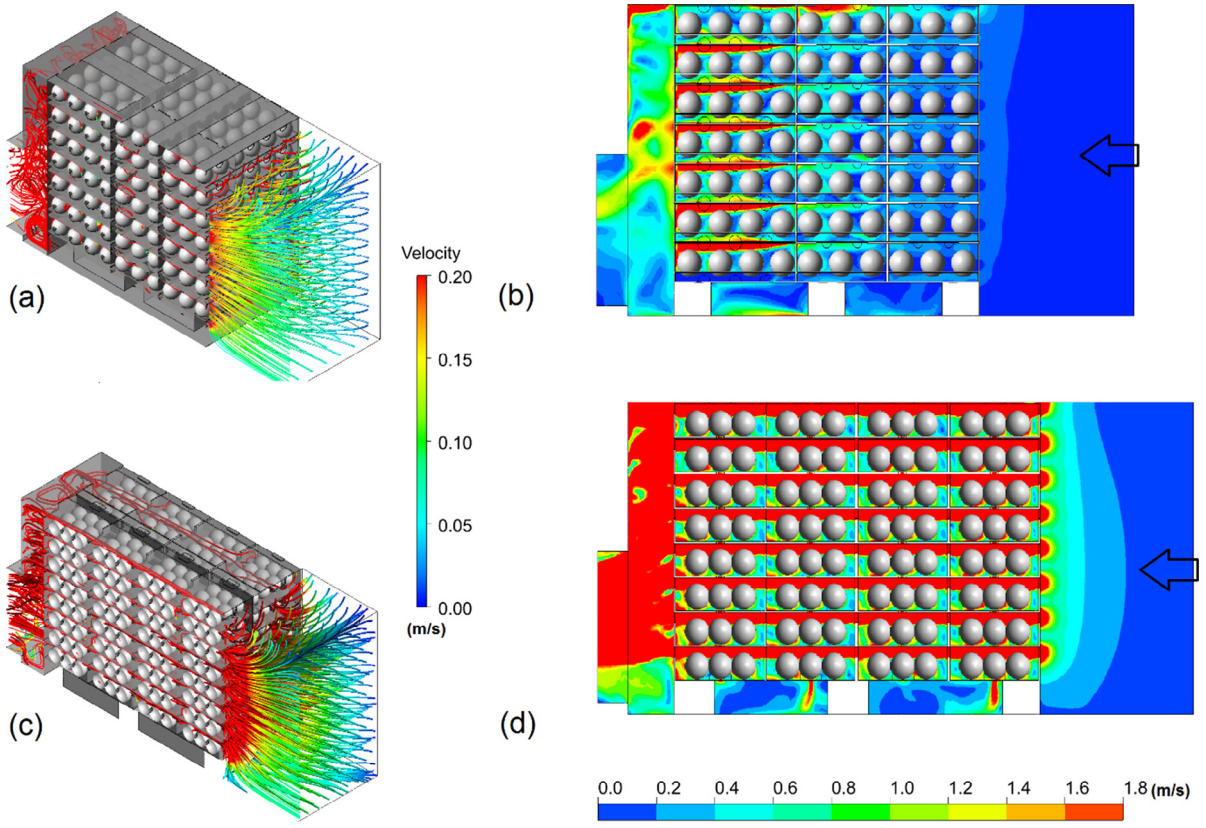

Fig. 10. Simulated stream lines of air velocity of the CT1 (a) and CT2 (c) stacks with no lining and contours of velocity on vertical plane sectioning the CT1 (b) and CT2 (d) stacks. Simulations were at air flow rate of 0.5 L kg^{-1} s^{-1}.

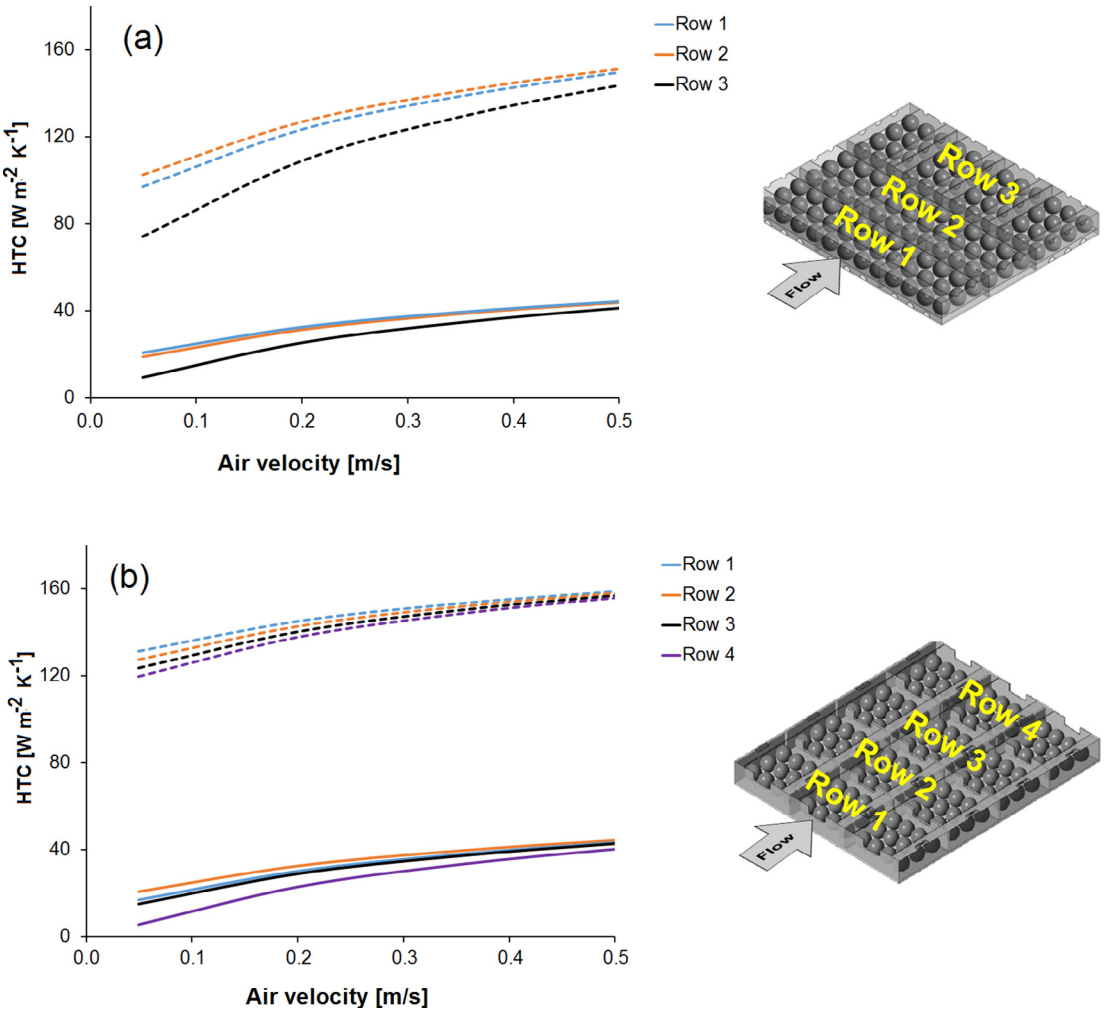

Fig. 11. Heat transfer coefficient (HTC) as a function of superficial air velocity through CT1 stack (a) and CT2 stack (b) with lining (full curves) and no lining (broken curves). Simulations correspond to FAC of pomegranates from 17 °C using cooling air at 7 °C.

fruit types. For instance, for carton of oranges or apple fruits, the contribution of the stacked fruit to the overall pressure loss would be relatively important (Verboven et al., 2006).

The model reproduced the actual position of the suction fan with respect to the stack. Hence, stream lines were captured as realistically as possible (Fig. 10(a) and (c)). The suction effect generated by the centrifugal fan draws refrigerated air horizontally through boxes at superficial air velocity of 0.13 and 0.17 m/s for the CT1 and CT2 stacks, respectively. Near vent-holes air velocity reached up to 5 m/s.

From the images of the velocity field inside the stack (Fig. 10 (b) and (d)), it is clear that airflow distribution depended on box design and box arrangement. Due to change in orientation of boxes, between the 2nd and 3rd row of the CT1 stack, vent openings were not line up from inlet to outlet. For this stack, vent-hole proportion, perpendicular to the airflow path, were 9.45% at inlet and outlet of the 1st row. Then, due to blockage of vent openings, it decreased to 2.15% at outlet from the 2nd row/ inlet to the 3rd row. This resulted a high local air velocities in the region above fruits in the 3rd row. In the CT2 stack, vent openings were perfectly lined up from inlet to outlet, forming tunnel like path through the stack.

3.3. Analysis of the cooling heterogeneity

Calculated value of surface averaged heat transfer coefficients (HTCs) are presented in Fig. 11. The HTCs were calculated from a steady state simulation of FAC of pomegranates from an initial pulp temperature of 17 °C at cold air temperature of 7 °C. For the range of airflow rates (from 0.05 to 0.5 m s^{-1}) the HTC ranged from 74 W m^{-2} to 159 W m^{-2} for stack with no liner and from 9.3 W m^{-2} to 48 W m^{-2} for stack with liner of the CT1 stack. Similarly, for the CT2 stack HTCs ranged from 120 W m^{-2} to 163 W m^{-2} for stack with no liner and from 5 W m^{-2} to 48 W m^{-2} for stack with liner. Hence, in average, plastic liners amounted to a reduction of HTC by 74%. Heat transfer coefficient increases with airflow and the distribution followed the airflow profile discussed previously. The relatively low heat transfer coefficient of the 3rd row of the CT1 stack is apparent.

Contours of instantaneous temperature distributions in a layer of the stacks with no plastic liner are presented in Fig. 12. The two box designs have distinctly different temperature distributions. The CT1 stack show wide variation of cooling rate between rows, with the 2nd row the fastest cooling and the 3rd row the slowest cooling. In the CT2 stack, fruits along the channelled flow path cool in a noticeably higher rate than fruits at the left and right of the airflow path.

Figs. 13 and 14 show temperature contours on outer plastic surfaces and on horizontal plane sectioning the stacks. The model enables to visualize and quantify temperatures of the free air, air inside the liners and the pomegranates. The insulation effect of the plastic liner is evident from the temperature difference between the free air and the air inside the liners. The pattern of

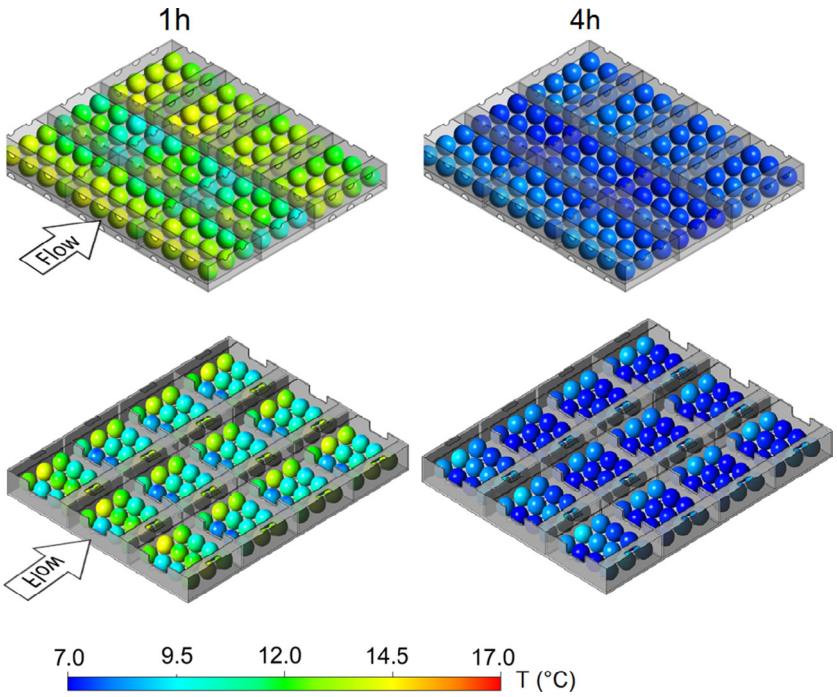

Fig. 12. Simulated contour of temperature distribution in a layer of CT1 (top row) and CT2 (bottom row) stacks with no lining. Simulation corresponds to an airflow rate of 0.5 L kg^{-1} s^{-1} at 7 °C. Contours were taken at 1 h (left column) and 4 h (right column).

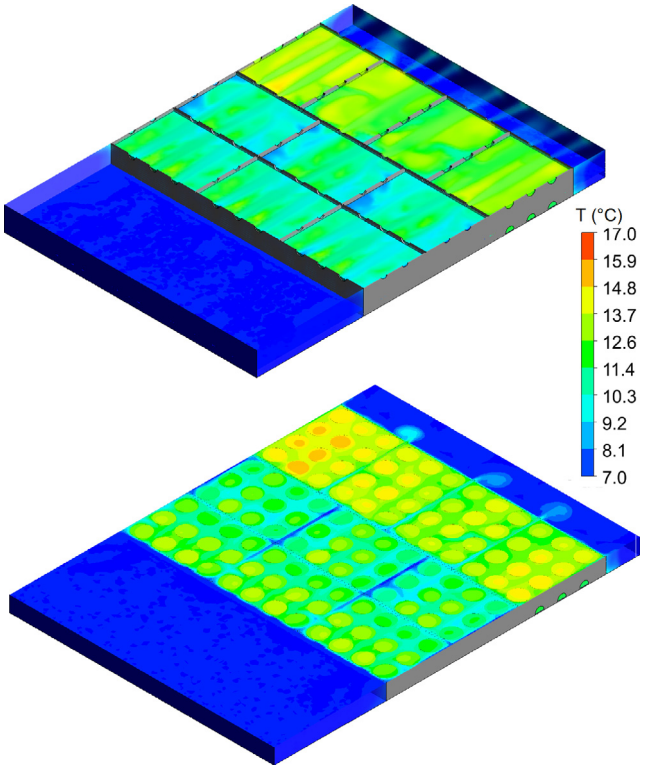

Fig. 13. Simulated contour of temperature distribution in a layer of CT1 stacks with lining. Instantaneous temperature contour on surface of plastic liner (top) and on horizontal plane through the stack (bottom). Simulation corresponds to an airflow rate of 0.5 L kg^{-1} s^{-1} at 7 °C. Contours were taken at 1 h.

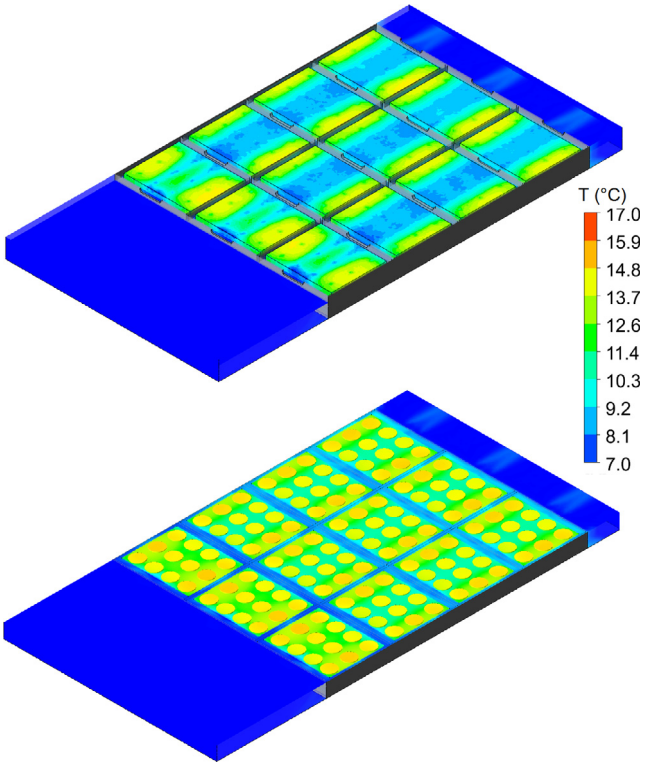

Fig. 14. Simulated contour of temperature distribution in a layer of CT2 stacks with lining. Temperature contour on surface of plastic liner (top) and contour on horizontal plane through the stack (bottom). Simulation corresponds to airflow rate of 0.5 L kg^{-1} s^{-1} at 7 °C. Contours were taken at 1 h.

temperature distribution inside the stack followed the trend observed for the no lining counterpart. Plastic lining decreased cooling rate without noticeably changing the pattern of high and low temperature regions. For both with and without lining cases, the rate of cooling vary significantly between rows in layer of the CT1 stack and between fruits in a box for the CT2 stack.

4. Conclusions

In this study, experiments and numerical simulation using the computational fluid dynamics code of ANSYS® CFX™ were carried out to characterize pressure loss, airflow patterns, and temperature distributions during forced-air precooling of pomegranate fruit.

Experiments and simulations highlighted the importance of package design and added packaging material like plastic lining on the airflow and cooling performances. Number of fruits per box were relatively few and pomegranates are loosely packed that pressure loss inside a box is minimum. Rather, pressure loss due to sudden contraction and expansion of the airflow path as air enters and leaves individual boxes in a stack is dominant. Hence, in FAC of pomegranate fruit, modification of package design can have significant influence on the aerodynamic and thermodynamic performances.

During precooling of palletized pomegranate, the high and low temperature regions depends considerably on package design. Especially during long storage of pomegranates or during long distance transportation, monitoring critical regions inside the stack would be very crucial for proper control of the cooling process. As clearly demonstrated in this study, critical regions depends on packaging design.

Liner is essential for postharvest handling of pomegranate. It reduces weight loss from fruit by acting as a barrier to moisture transport from fruit to the bulk air. However, it increased airflow resistance and reduced convective heat transfer from produce, leading to increased cooling time and energy use. With liners being the most decisive factor affecting cooling rate and energy consumption of the cooling process, it is interesting to study the effect of adding perforations on liners.

Acknowledgements

This work is based upon research supported by the South African Research Chairs Initiative of the Department of Science and Technology and National Research Foundation. The financial support of the pomegranate Growers' Association of South Africa (POMASA) and the Postharvest Innovation Programme (PHI) through the award of research grant to Prof. U.L. Opara are gratefully acknowledged.

References

Ambaw, A., Delele, M., Defraeye, T., Ho, Q., Opara, U.L., Nicolai, B.M., Verboven, P., 2013. The use of CFD to characterize and design post-harvest storage facilities: Past, present and future. Comput. Electron. Agric. 93, 184–194.

Anderson, B.A., Sarkar, A., Thompson, J.F., Singh, R.P., 2004. Commercial scale forced air cooling of strawberries. Trans. ASAE 47 (1), 183–190.

Akdemir, S., Arin, S., 2006. Spatial variability of ambient temperature, relative humidity and air velocity in a cold store. J. Cent. Eur. Agric. 7 (1), 101–110.

Alvarez, G., Flick, D., 1999a. Analysis of heterogeneous cooling of agricultural products inside bins – Part I: Aerodynamic study. J. Food Eng. 39, 227–237.

Alvarez, G., Flick, D., 1999b. Analysis of heterogeneous cooling of agricultural products inside bins – Part II: Thermal study. J. Food Eng. 39, 239–245.

Artés, F., Marín, J.G., Martínez, J.A., 1996. Controlled atmosphere storage of pomegranate. Zeitschrift für Lebensmittel-Untersuchung und Forschung 203, 33–37.

Artés, F., Tudela, J.A., Villaescusa, R., 2000. Thermal postharvest treatments for improving pomegranate quality and shelf life. Postharvest Biol. Technol. 18 (3), 245–251.

Berry, T., Delele, M.A., Griessel, H., Opara, U.L., 2015. Geometric design characterisation of ventilated multi-scale packaging used in the South African pome fruit industry. Agric. Mech. Asia, Africa, Latin Am. 46 (3), 34–42.

Berry, T.M., Defraeye, T., Nicolai, B.M., Opara, U.L., 2016. Multiparameter analysis of cooling efficiency of ventilated fruit cartons using CFD: impact of vent hole design and internal packaging. Food Bioprocess Technol. 9, 1481. http://dx.doi.org/10.1007/s11947-016-1733-y.

Choi, Y., Okos, M.R., 1986. Effects of temperature and composition on the thermal properties of foods. In: LeMaguer, M., Jelen, P. (Eds.), Food Engineering and Process Applications, vol. 1. Elsevier Applied Science, London, pp. 93–101.

Defraeye, T., Lambrecht, R., Tsige, A.A., Delele, M.A., Opara, U.L., Cronjé, P., Verboven, P., Nicolai, B.M., 2013. Forced-convective cooling of citrus fruit: package design. J. Food Eng. 118, 8–18.

Delele, M.A., Tijskens, E., Atalay, Y.T., Ho, Q.T., Ramon, H., Nicolai, B.M., Verboven, P., 2008. Combined discrete element and CFD modelling of airflow through random stacking of horticultural products in vented boxes. J. Food Eng. 89 (1), 33–41.

Delele, M.A., Ngcobo, M.E.K., Getahun, S.T., Chen, L., Mellmann, J., Opara, U.L., 2013. Studying airflow and heat transfer characteristics of a horticultural produce packaging system using a 3-D CFD model. Part I: Model development and validation. Postharvest Biol. Technol. 86, 536–545.

Fawole, O.A., Opara, U.L., 2013. Effects of storage temperature and duration on physiological responses of pomegranate fruit. Ind. Crops Prod. 47, 300–309.

Ferrua, M.J., Singh, R.P., 2009. Modeling the forced-air cooling process of fresh strawberry packages, Part I: Numerical model. Int. J. Refrig. 32, 335–348.

Franke, J., Hellsten A., Schlünzen, H., Carissimo, B., 2007. Best practice guideline for the CFD simulation of flows in the urban environment. COST Action 732: Quality Assurance and Improvement of Microscale Meteorological Models, Hamburg, Germany.

Gil, R., Bojaca, C.R., Schrevens, E., Suay, R., 2012. Analysis of air temperature distribution inside a cold store by means of geostatistical methods. In: 4th International Conference on Postharvest Unlimited, Leavenworth, WA. Acta Hortic. 945, 29–37.

Harper, C.A., 2004. Handbook of Building Materials for Fire Protection. McGraw-Hill, New York (pp. 7–1).

Ho, S.H., Rahman, M.M., Sunol, A.K., 2010. Analysis of thermal response of a food self-heating system. Appl. Therm. Eng. 30 (14), 2109–2115.

Kader, A.A., Chordas, A., Elyatem, S., 1984. Response of pomegranates to ethylene treatment and storage temperature. Calif. Agric. 38, 14–15.

Köksal, I., 1989. Research on the storage of pomegranate cv. 'Gökbahçe' under different conditions. Acta Hort. 258, 295–302.

Mangaraj, S., Goswami, T.K., Mahajan, P.V., 2009. Applications of plastic films for modified atmosphere packaging of fruits and vegetables: a review. Food Eng. Rev. 1 (2), 133–158.

Menter, F.R., 1994. Two-equation eddy-viscosity turbulence models for engineering applications. AIAA J. 32 (8), 1598–1605.

Mertens-Talcott, S.U., Jilma-Stohlawetz, P., Rios, J., Hingorani, L., Derendorf, H., 2006. Absorption, metabolism, and antioxidant effects of pomegranate (Punica granatum L.) polyphenols after ingestion of a standardized extract in healthy human volunteers. J. Agric. Food Chem. 54 (23), 8956–8961.

Mirdehghan, S.H., Rahemi, M., Martínez-Romero, D., Guillén, F., Valverde, J.M., Zapata, P.J., Serrano, M., Valero, D., 2007. Reduction of pomegranate chilling injury during storage after heat treatment: role of polyamines. Postharvest Biol. Technol. 44 (1), 19–25.

Mirdehghan, S.H., Rahemi, M., Serrano, M., Guillén, F., Martínez-Romero, D., Valero, D., 2006. Prestorage heat treatment to maintain nutritive and functional properties during postharvest cold storage of pomegranate. J. Agric. Food Chem. 54 (22), 8495–8500.

Munhuweyi, K., Lennox, C.L., Meitz-Hopkins, J.C., Caleb, O.J., Opara, U.L., 2016. Major diseases of pomegranate (Punica granatum L.), their causes and management—a review. Sci. Hortic. 211, 126–139.

Norton, T., Da-Wen, Sun, 2006. Computational fluid dynamics (CFD) – an effective and efficient design and analysis tool for the food industry: a review. Trends Food Sci. Technol. 17, 600–620.

Ngcobo, M.E., Delele, M.A., Opara, U.L., Zietsman, C.J., Meyer, C.J., 2012. Resistance to airflow and cooling patterns through multi-scale packaging of table grapes. Int. J. Refrig. 35 (2), 445–452.

Opara, L.U., Zou, Q., 2007. Sensitivity analysis of a CFD modelling system for airflow and heat transfer of fresh food packaging: inlet air flow velocity and inside – package configurations. Int. J. Food Eng. 3 (5), 1556–3758. http://dx.doi.org/10.2202/1556-3758.1263. ISSN (Online).

Onur, C., Pekmezci, M., Tibet, H., Erkan, M., Kuzu, S., 1995. Investigations on pomegranate storage. Second Turkish National Horticultural Congress, 3–6 October, 1, pp. 696–700.

Opara, U.L., 2011. From Hand Holes to Vent Holes: What's Next in Innovative Horticultural Packaging? Inaugural Lecture. Stellenbosch University, South Africa, p. 24p.

Opara, U.L., Atukuri, J., Fawole, O.A., 2015. Application of physical and chemical postharvest treatments to enhance storage and shelf life of pomegranate fruit – a review. Sci. Hortic. 197, 41–49.

Pareek, S., Valero, D., Serrano, M., 2015. Postharvest biology and technology of pomegranate. J. Sci. Food Agric. 95 (12), 2360–2379.

Roache, P.J., 1994. Perspective: a method for uniform reporting of grid refinement studies. Trans. ASME – J. Fluids Eng. 116 (3), 405–413.

Seeram, N.P., Schulman, R.N., Heber, D., 2006. Pomegranates: ancient roots to modern medicine. Medicinal and Aromatic Plants—Industrial Profiles, vol. 43. CRC/Taylor & Francis, Boca Raton.

Smale, N.J., Moureh, J., Cortella, G., 2006. A review of numerical models of airflow in refrigerated food applications. Int. J. Refrig. 29, 911–930.

USDA, 1996. Nutrient Database for Standard Reference. U.S. Department of Agriculture, Washington, D.C..
Verboven, P., Flick, D., Nicolai, B.M., Alvarez, G., 2006. Modelling transport phenomena in refrigerated food bulks, packages and stacks: basics and advances. Int. J. Refrig. 29 (6), 985–997.
Viuda-Martos, M., Fernández-López, J., Pérez-Álvarez, J.A., 2010. Pomegranate and its many functional components as related to human health: a review. Compr. Rev. Food Sci. Food Safety 9 (6), 635–654.
Zou, Q., Opara, L.U., McKibbin, R., 2006a. A CFD modeling system for airflow and heat transfer in ventilated packaging for fresh foods I: Initial analysis and development of mathematical models. J. Food Eng. 77 (4), 1037–1047.
Zou, Q., Opara, L.U., McKibbin, R., 2006b. A CFD modeling system for airflow and heat transfer in ventilated packaging for fresh foods II: computational solution, software development and model testing. J. Food Eng. 77 (4), 1048–1058.